Proceedings of the 3rd IASME/WSEAS Int. Conf. on HEAT TRANSFER, THERMAL ENGINEERING AND ENVIRONMENT, Corfu, Greece, August 20-22, 2005 (pp141-146)

Experiments on Visualizing the pseudo-3D Structure of Bubble Shape and its Surrounding Liquid Motion

YUKI MIYAMOTO and TAKAYUKI SAITO
Department of Mechanical Engineering
Shizuoka University
3-5-1 Johoku, Hamamatsu, Shizuoka 432-8561
JAPAN
ttsaito@ips.shizuoka.ac.jp http://flow.eng.shizuoka.ac.jp

Abstract: - The interface motion of a bubble and the structure of the surrounding liquid motion were simultaneously visualized to obtain their relationship. A zigzag rising bubble of 2.66 mm in equivalent diameter was examined in a rest water column. The bubble shape was filmed using illumination imaging technique with a red LED. On the other hand, the structure of the surrounding liquid motion was visualized via PIV and LIF (Particle Image Velocimetry and Laser Induced Fluorescence). Two sets of CCD camera simultaneously captured the bubble shape and liquid motion. The bubble image and tracer particles were superimposed into one frame. In addition, using a high-resolution CCD camera in space, we overcame the demerit of low time resolution in the conventional PIV measurements. The pseudo-3D flow structure was quantitatively reconstructed on the basis of 2D PIV results as well as 3D bubble shape. Our experimental results showed that the curvature of the outside at the inversion point of the zigzagging motion was larger than that of the inside; the vorticity of the outside at the inversion point was also larger than that of the inside. These two parameters periodically fluctuate and have been distinctively coupled with each other.

Key-Words: - Multiphase Flow, PIV, LIF, Single bubble, Shape deformation, Wake, Experiments

1 Introduction

Gas-liquid-multiphase systems are encountered in the broad field from advanced industries to the global environment. The global warming caused by greenhouse gases is one of the most serious human influences. For the purpose of mitigating the sudden increase of the atmospheric CO_2 concentration, Gas Lift Advanced Dissolution (*GLAD*) system [1] [2] [3] has been proposed; hence fundamental studies on this system have been conducted [4] [5] [6]. In order to improve its operation efficiency, the control of CO_2-bubble dissolution is needed. For achievement of this purpose, we have to elucidate the dynamic mechanism of mass transfer across the oscillating gas-liquid interface. Through the microscopic analysis of the motion of a single ascending bubble, we have been deepening understanding of the motion of the bubble and its surrounding liquid. The dissolution of CO_2, *i.e.* the mass transfer coefficient for a single bubble, depends on the bubble diameter [7]. The optimum bubble size is about 2mm for the *GLAD* system. At this time, the mass transfer coefficient for CO_2 becomes the maximum experimentally. In order to design a practical system, we elucidate the more details of the motion of the rising bubbles in the range from 2 to 5 mm in equivalent diameter. For the bubbles in such range, it is well known that their ascent trajectories are zigzagging and/or helical paths [8]. Trying to elucidate these mechanisms, many studies had been conducted from last half century. Nowadays, Laser devices such as Laser Doppler Anemometer (LDA), Particle Image Velocimetry (PIV) and so on, have enabled researchers to obtain more detailed bubble shape and the flow structure.

Ellingsen and Risso [9] used LDA combined with two sets of cameras to provide simultaneous measurements for the bubble motion and the flow structure of surrounding liquid. Both the gas and liquid phases had been accurately investigated, however the description about interface motion of the bubble might not be detailed. Brücker [10] implemented PIV; he mentioned the bubble shape and liquid velocity field. Recently, Fujiwara *et al.* [11] investigated the flow structure in the vicinity of a bubble moving in a shear flow via combination of PIV-LIF and shadow image technique. Tomiyama *et al.* [12] reported that a terminal velocity of an isolated single bubble depends on the initial shape deformation. Wu and Gharib [13] obtained the similar knowledge. Although many researches have been discussing the behaviour of the

single bubble in a liquid phase, the knowledge about the relationship between the bubble and liquid motion is still insufficient. As mentioned above, the purpose of this study is to elucidate the coupling mechanism between the interface motion of the bubble and the motion of its surrounding liquid. We focused on the local scale structure of the liquid and microscopic motion of the bubble interface. The position of measurement area was shifted at camera-subject depth; hence we can obtain the pseudo-3D flow structure of the liquid phase. In addition, the 3D bubble shape was reconstructed by visualizing two perpendicular images, and is investigated in detail.

2 Experimental method

The isolated single bubble was forced the rising motion by its own buoyancy. The liquid motion induced by the bubble buoyancy was visualized via PIV-LIF system. In order to remove the light scattered from the bubble and detect the tracer particles near the bubble interface, we employed Laser Induced Fluorescence (LIF) method [14]; the tracer was a fluorescence particle (Rhodamine-B, excitation 530-542nm, emission 575nm), and is approximately 50μm diameter. Figure 1-a shows the experimental setup used in the present investigation. Figure 1-b illustrates the top view of the setup. Three sets of high-resolution CCD camera, double-pulse Nd-YAG laser and two red LED were arranged precisely. The motion of bubble interface and liquid was visualized simultaneously. Deionized and boiled-out water was filled to a depth of 270mm in an acrylic water vessel of 150-mm-cross section. A pure air bubble was released from a hypodermic needle (0.40mm of inner diameter) located at the center of the bottom under the condition of constant flow rate and pressure. A single bubble was released from the needle tip at regular interval of about 3 seconds. Under this condition, the wake of the leading bubble doesn't affect the trailing bubble. In our study, the bubble has the two-dimensional zigzag trajectory. We defined that the *x*-*y* plane corresponded with zigzagging plane, and its orthogonal plane was the *y*-*z* plane.

In order to obtain the bubble diameter, we measured the volume of 200 bubbles trapped directly using a small glass bottle. As a result, the mean volume-equivalent diameter was 2.66mm. This bubble was much larger than needle's inner diameter of 0.40mm, inevitably it can be categorized into the *large initial deformation* [12] [13]. We can consider that the initial shape was dominant factor for subsequent fate of the bubble. We were appropriately adjusted to the pressure and flow rate so that the bubble might have the zigzag trajectory. These bubbles showed almost the same shape and the ascent motion. Therefore, the high reproducible measurement was performed; and the statistical analysis of the motion of the bubbles is considered to be reasonable. The flow structure of the liquid around the bubble was measured using PIV (TSI PIV-CAM, 1000×1016pixel^2); hence we quantitatively obtained the velocity field. Simultaneously, the interface motion of the bubble was captured from opposite direction of PIV with the CCD camera-A (Hitachi KP-F110, 1k×1kpixel^2,

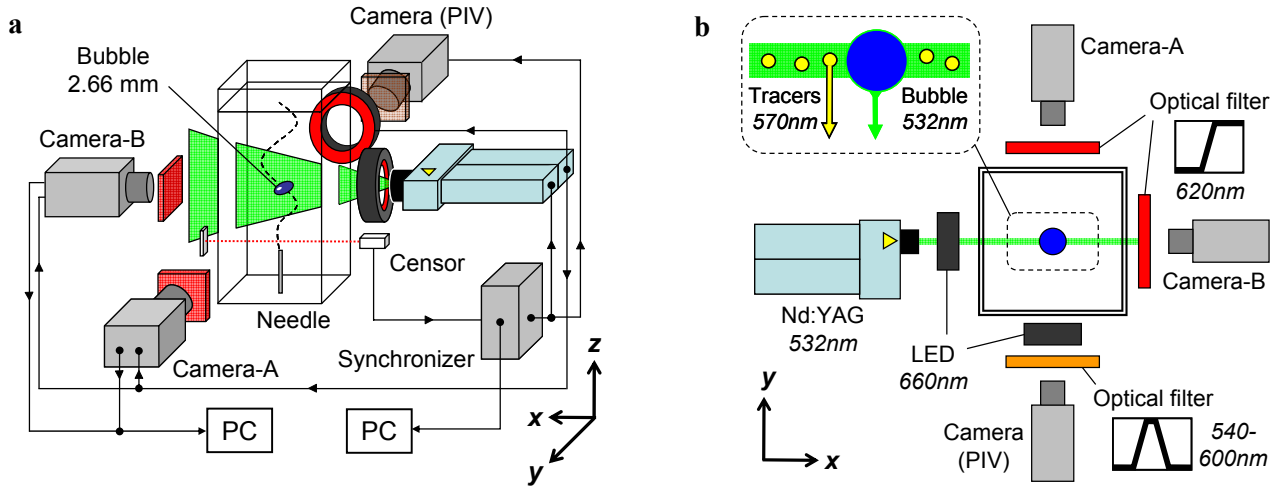

Fig. 1 Schematic of experimental setup

exposure time 200μs). This camera filmed images of illuminated bubble contour by red LED pulse (660nm). There were distinguished differences between the excitation emission of fluorescence particles (570nm) and the scattered light from the bubble surface (532nm). Therefore, CCD camera for PIV easily detected only tracers using an optical filter (540-600nm). More detailed data in the vicinity of the bubble surface was obtained.

In order to obtain the pseudo-3D flow structure of the liquid-phase motion, the laser-sheet whose thickness is about 1mm was shifted at intervals of 1mm. The shift of YAG-laser made it possible to obtain velocity information of each cross section. The CCD camera-B (the same as camera-A) was used to confirm positional relationship between bubble and laser sheet. Both camera-A and -B were equipped with the optical filter which can reduce YAG-laser emission. A shady area developed behind the bubble, a mirror (omitted in Figure 1-a) was arranged to eliminate bubble's shadow. An optical laser passing sensor was implemented as trigger for starting record, and a synchronizer and a PC controlled these apparatuses. Figure 2 shows the timing diagram. The interval of double pulse was 300μs; two LED light were emitted for this time, and the bubble was filmed instantaneously. 100 bubbles were filmed in each position, and the results were averaged. The uncertainty of the velocity of the liquid was analyzed to be U_{95}=6.2mm/s. Moreover, these measurements were carried out from mutually perpendicular two directions in order to obtain more detailed information about the bubble shape. The expanded uncertainty of the average center of gravity coordinate of the bubble was estimated to be U_{95}=0.067mm.

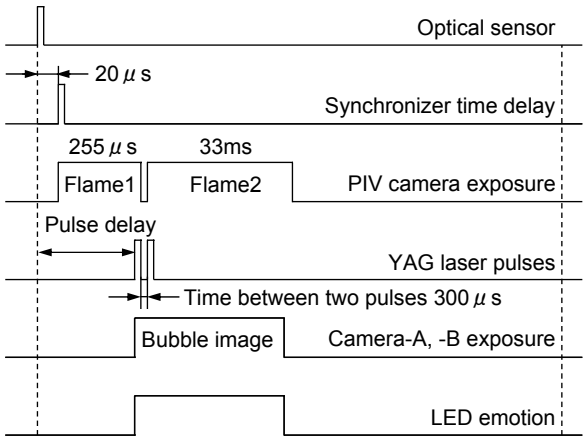

Fig. 2 Timing diagram of measurements

3 Results and Discussion

3.1 Bubble shape deformation

An image analysis of bubble images was processed, and the bubble's parameter such as the center of gravity, the major and minor axes, the contour and so on, was calculated. As the pixel size was 9.74μm, we obtained the high-resolution in space. The ascending velocity of the center of gravity was approximately 300mm/s, therefore *Re*, *We* and *Eo* numbers (Refer to Bhaga and Weber [15]) were 800, 3.3 and 0.95, respectively. The basic bubble shape was categorized into a type of oblate spheroid. The origin of coordinates is set as the needle tip. The measuring points were six in total; P1(z = 12.0), P2(z = 22.2), P3(z = 36.7), P4(z = 48.1), P5(z = 65.1) and P6(z = 77.1). P3 and P5 are the inflection points; P4 and P6 are the inversion points at which the bubble itself changes the direction on the zigzag path. Figure 3 shows the bubble trajectory and reconstructed 3D bubble shape. Filming images from orthogonal two directions and assuming that the bubble shape in the x-y cross section is a circle mostly, 3D shape of the bubble can be reconstructed. The major and minor axes of this ellipsoid were defined as the major axes of bubble shape projection on the x-z and y-z planes. The validity for such assumption is substantiated by the past visualization results that the cross-sectional shape showed the approximate circle [16]. In an x-z plane, the bubble ascended zigzagging, while its trajectory was almost rectilinear in a y-z plane. The average volume of the reconstructed bubble was 10.64mm^3, and it was almost the same as the result from the direct sampling.

At P3 and P5 (*i.e.*, the inflection points), the remarkable tilting of the bubble was observed as clearly shown in Figure 3. These shadow images of the largely-tilting bubble bring down superficially large shape deformation to an observer. However, it is clear that the bubble was not significantly deformed as compared with the superficial deformation actually. The bubble shape had the asymmetrical property at the inversion points (P4 and P6). As the radius of curvature at left and right side edges of the bubble contour (r_{left} and r_{right}) was measured, r_{left} is 0.59mm and r_{right} was 0.40mm at P4. On the other hand, r_{left} was 0.39mm and r_{right} is 0.55mm at P6. As a result, the asymmetric of the shape deformation was estimated quantitatively. The important point to note is that the radius of curvature at the inside edge of the trajectory was larger than that of the outside edge. This asymmetric is due to the fluctuation of the ambient

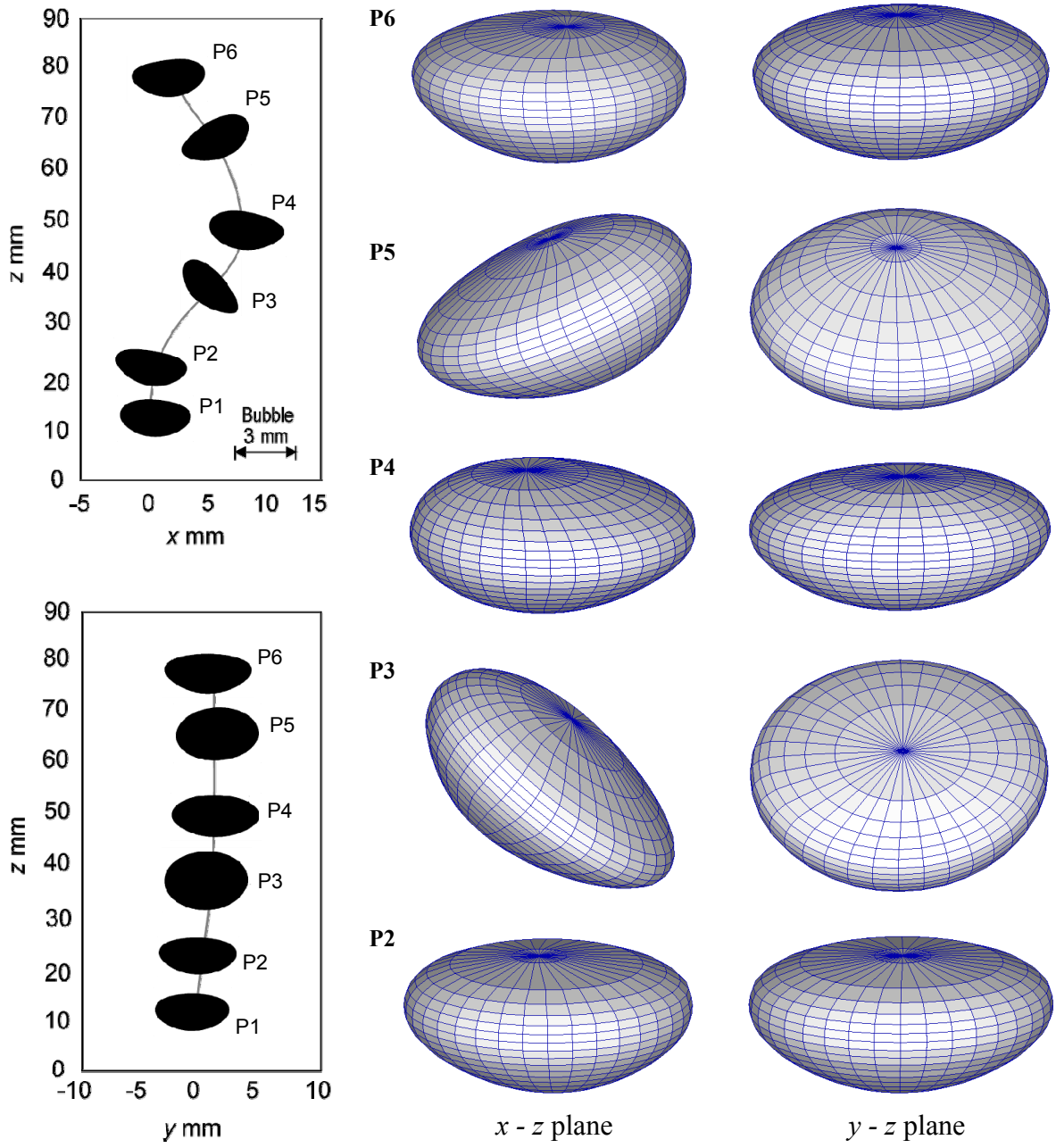

Fig. 3 Reconstructed 3D bubble shapes and ascent trajectories

pressure which was influenced by the vortex shedding.

3.2 Flow structure induced the bubble

Figures 4 and 5 show the pseudo-3D flow structure around the bubble at P6 which is second inversion point. These figures reveal the positional relation between the center of gravity of the bubble and the laser-sheet, the distribution of the average velocity vectors on the *x*-*z* (*y*-*z*) plane and the contour map of the average vorticity. In Figure 4-c and Figure 5-h, one can see, from the instantaneous velocity fields, that the flow structure of the liquid-phase streaming from the frontal- to rear-side of the bubble is developing. The vorticity distribution on *x*-*z* plane has been found to be asymmetry at left-and-right side in the vicinity of the bubble surface. In the wake on the *x*-*z* plane, the intensity of positive vorticity became larger than the negative one; *i.e.* it indicates that vorticity developed more intensively at the outside of the bubble trajectory

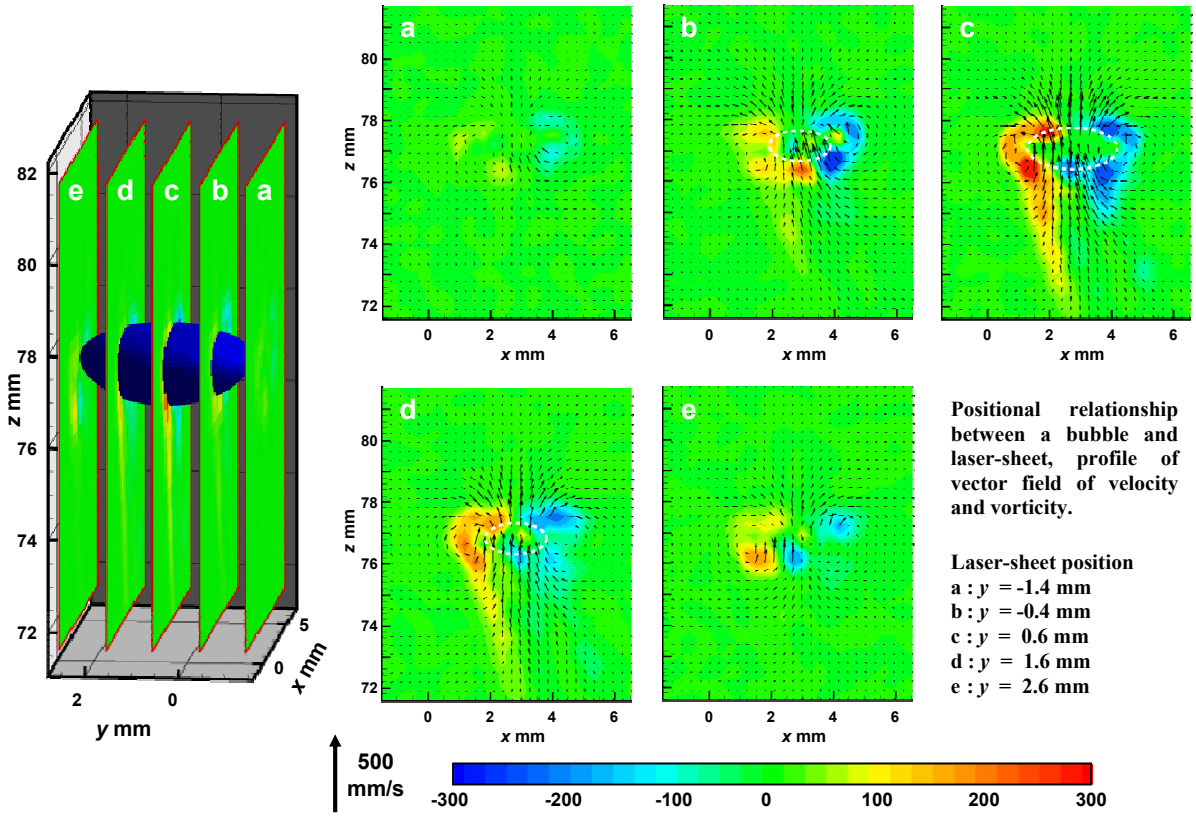

Fig. 4 Contour map of vorticity on $x - z$ plane at the second inversion point (P6)

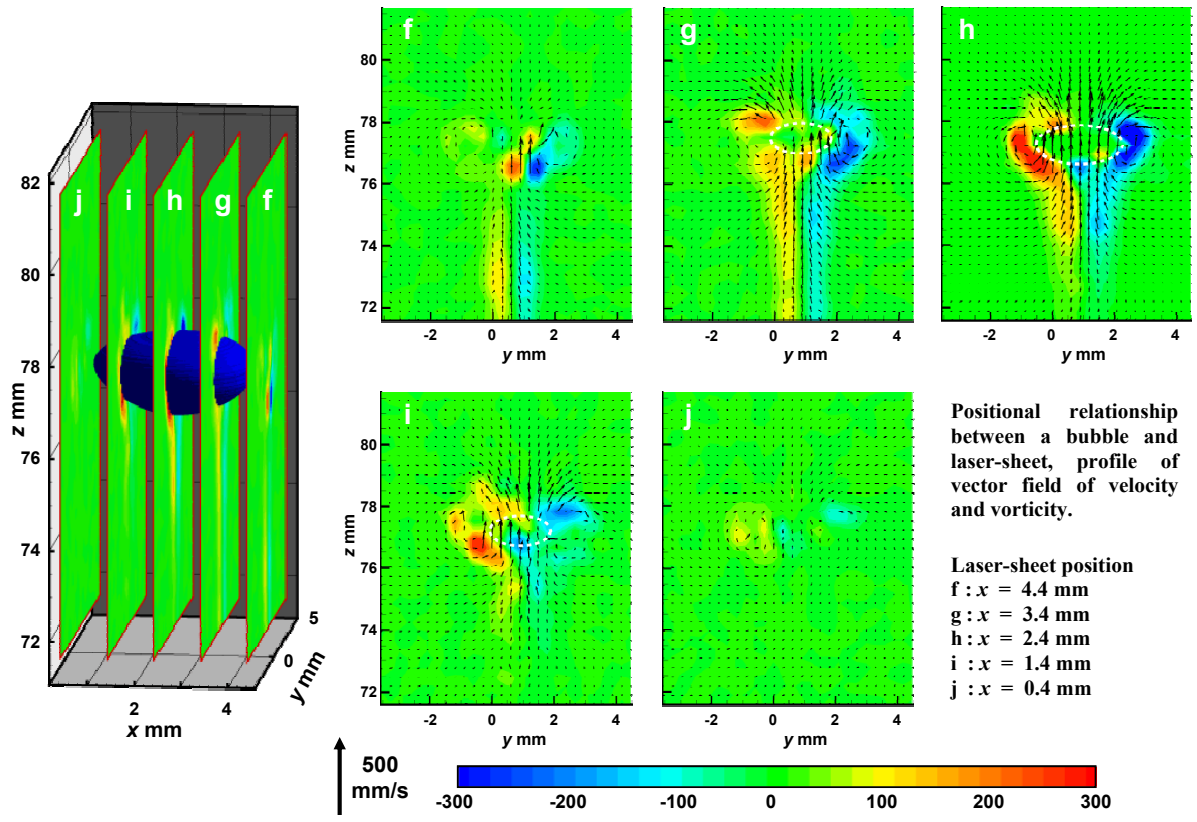

Fig. 5 Contour map of vorticity on $y - z$ plane at the second inversion point (P6)

than the inside. The opposite phenomenon was observed at the first inversion point. On the contrast, the flow structure has been found to be symmetric on the *y-z* plane. This result made it evident that the surrounding liquid motion has the plane-symmetry with respect to the zigzagging plane.

As leaving the center of the bubble, both velocity vector and vorticity became weak gradually. When the interval between the laser-sheet and bubble was about 3mm, the liquid motion was hardly observed. (These figures were omitted.) However, the incorrect vectors can appear despite the long distance from the bubble. These should be considered to be the apparent error due to the intensive light scattered from the bubble interface, therefore the magnitude of the error vectors was almost the same as the bubble velocity. Although the optical band-pass filter was attached to the front of PIV camera, YAG-laser can't be cut off completely. Consequently, judging the incorrect vectors using both the magnitude of the error vectors and the coordinates of scattering noise on raw images, these errors were removed.

4 Conclusion

The isolated bubble of 2.66mm in equivalent diameter rising in reset water was investigated by PIV-LIF system and high-speed CCD cameras. In order to obtain the pseudo-3D flow structure, the test section was shifted at the interval of about 1mm. In addition, 3D bubble shape was reconstructed; hence the shape deformation had the asymmetry on the zigzagging motion plane, and the symmetry on its orthogonal plane. The future direction of this study will be more detail investigation for 3D flow structure, and the analysis of an unsteady wake.

References:

[1] Saito, T., Kajishima, T. and Nagaosa, R., CO_2 Sequestration at sea by gas-lift system of shallow injection and deep releasing, *Environmental Sci. & Tech.*, 34, 2000, pp.4140-4145.

[2] Saito, T., Kosugi, S., Kajishima, T. and Tsuchiya, K., Characteristics and performance of a deep ocean disposal system for low-purity CO2 gas via a gas lift effect, *Energy & Fuels*, 15, 2001, pp.285-292.

[3] Saito, T., Kajishima, T. and Tsuchiya, K., Pumping characteristics of a large-scale gas-lift system, *Experimental Thermal & Fluid Science*, 28, 2004, pp.479-488.

[4] Saito, T., Kajishima, T., Tsuchiya, K. and Kosugi, S., Mass transfer and structure of bubbly flows in a system of CO_2 disposal into the ocean by gas-lift column, *Chem. Eng. Sci.*, 54, 1999, pp.4945-4951.

[5] Saito, T., Tsuchiya, K. and Kajishima, T., Local and global scale structure of bubbly flows in glad (gas lift advanced dissolution) system, *Exp. Thermal & Fluid Science*, 29, 2005, pp.305-313.

[6] Mudde, R. F. and Saito, T., Hydro -dynamical similarities between bubble column and bubbly pipe flow, *J. Fluid Mech.*, 437, 2001, pp.203-228.

[7] Motarjemi, M. and Jameson, G. J., Mass Transfer from very small bubbles-the optimum bubble size for aeration, *Chem. Eng. Sci.*, 33, 1978, pp.1415-1423.

[8] Clift, R., Grace, J. R. and Weber, M. E., Bubbles, Drops, and Particles. *Academic Press,* 1978.

[9] Ellingsen, K. and Risso, F., On the rise of an ellipsoidal bubble in water: oscillatory paths and liquid induced velocity, *J. Fluid Mech.*, 440, 2001, pp.235-268.

[10] Brücker, C., Structure and dynamics of the wake of bubbles and its relevance for bubble interaction, *Phys. Fluids* ,11, 1999, pp.1781-1796.

[11] Fujiwara, A., Danmoto, Y., Hishida, K. and Maeda. M., Bubble deformation and flow structure measured by double shadow images and PIV/LIF, *Exp. Fluids*, 36, 2004, pp.157-165.

[12] Tomiyama, A., Celata, G.P., Hosokawa, S. and Yoshida, S. Terminal velocity of single bubbles in surface tension force dominant regime, *Intl J. Multiphase Flow*, 28, 2002, pp.1497-1519.

[13] Wu, M. and Gharib, M., Experimental studies on the shape and path of small air bubbles rising in clean water, *Phys. Fluids* ,14, 2002, pp.L49-L52.

[14] Tokuhiro, A., Maekawa, M., Iizuka, K., Hishida, K. and Maeda, M., Turbulent flow past a bubble and ellipsoid using shadow-image and PIV tech -niques, *Intl J. Multiphase Flow*, 24, 1998, pp.1383-1406.

[15] Bhaga, D. and Weber, M. E., Bubbles in viscous liquids: shapes, wakes and velocities, *J. Fluid Mech.*, 105, 1981, pp.61-85.

[16] Miyamoto, Y., Saito, T., Kumagai, A. and Amma, S., Coupling mechanism of the motion of the center of gravity and the interface motion of a bubble zigzag rising in a rest water column, *The 10th APCChE congress*, Kitakyushu, Japan, 2004.